Biophysical Journal, Volume *115*

Supplemental Information

Water Distribution within Wild-Type NRas Protein and Q61 Mutants during Unrestrained QM/MM Dynamics

Ruth H. Tichauer, Gilles Favre, Stéphanie Cabantous, Georges Landa, Anne Hemeryck, and Marie Brut

General system properties

Figures S1 to S7 show general system properties extracted as a function of time during QM/MM dynamics simulations (potential, kinetic and total energy, density, temperature, pressure, volume and backbone RMSD versus time). Results are presented for WT NRas and Q61 mutants.

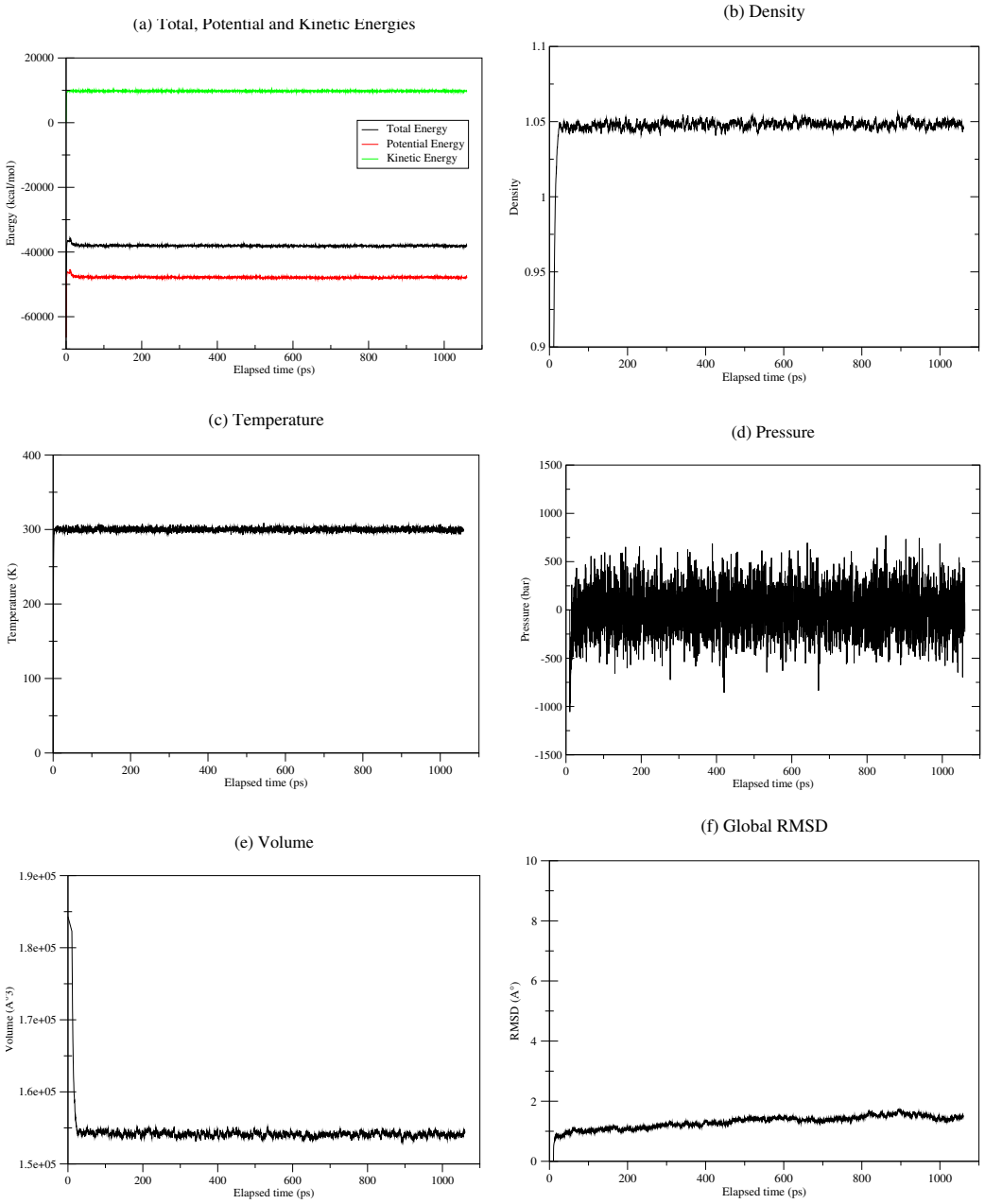

Figure S1: System properties as a function of time for wild type p21^{N-ras} during QM/MM dynamics simulations (a) Potential, kinetic and total energy (b) Density, (c)Temperature, (d) Pressure, (e) Volume and (f) backbone atoms rmsd.

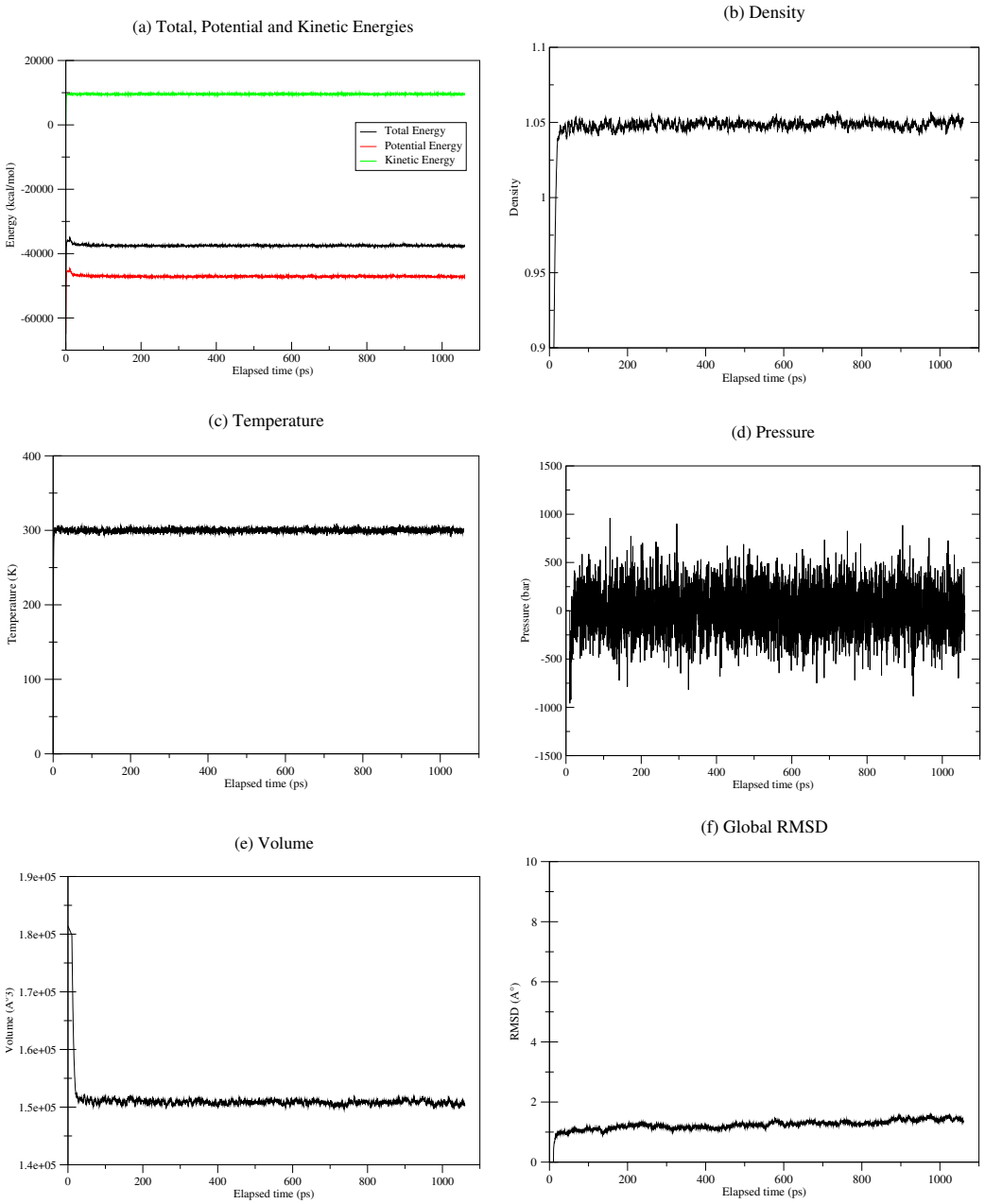

Figure S2: System properties as a function of time for Q61E NRas during QM/MM dynamics simulations (a) Potential, kinetic and total energy (b) Density, (c)Temperature, (d) Pressure, (e) Volume and (f) backbone atoms rmsd.

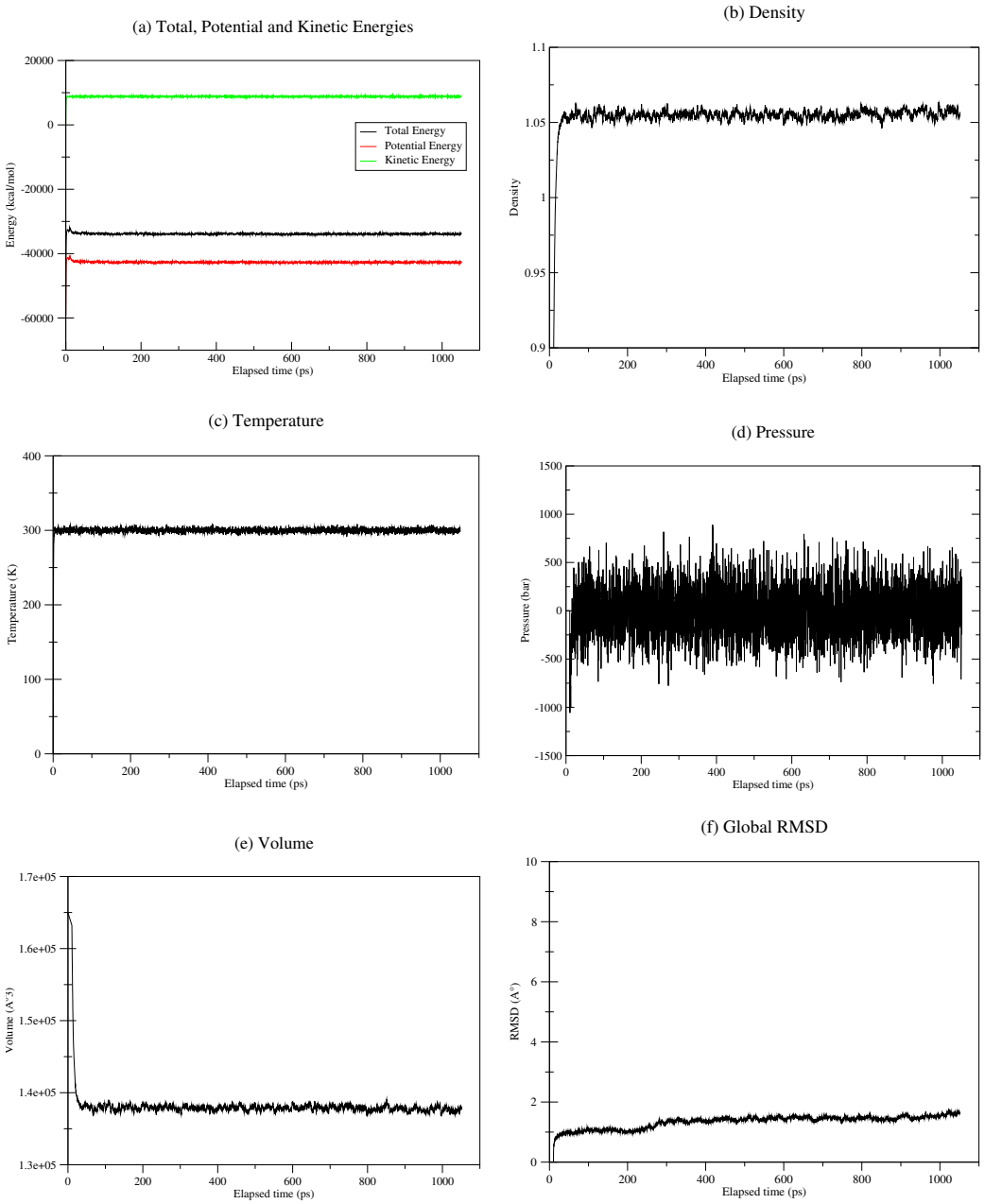

Figure S3: System properties as a function of time for Q61P NRas during QM/MM dynamics simulations (a) Potential, kinetic and total energy (b) Density, (c)Temperature, (d) Pressure, (e) Volume and (f) backbone atoms rmsd.

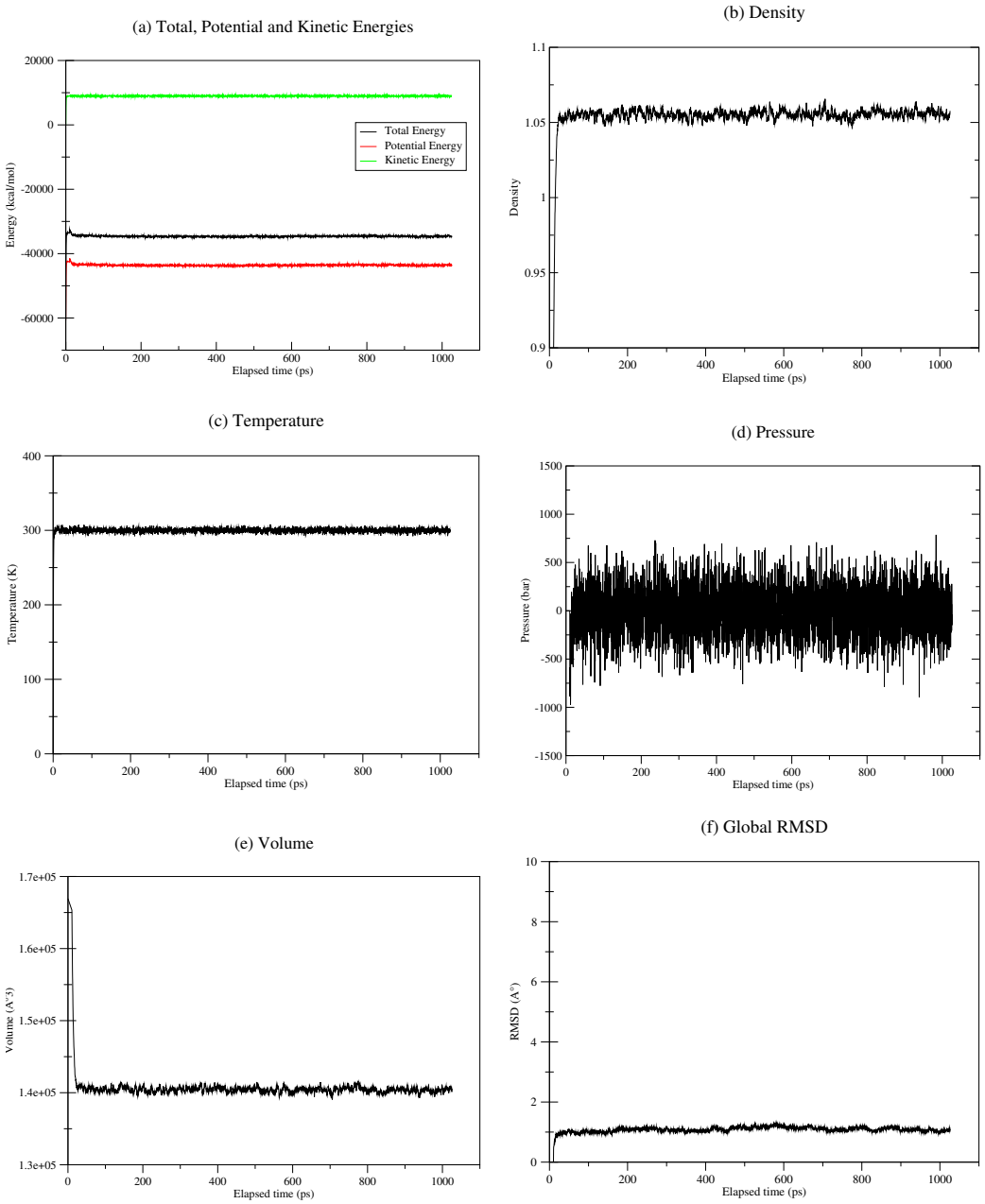

Figure S4: System properties as a function of time for Q61H NRas during QM/MM dynamics simulations (a) Potential, kinetic and total energy (b) Density, (c)Temperature, (d) Pressure, (e) Volume and (f) backbone atoms rmsd.

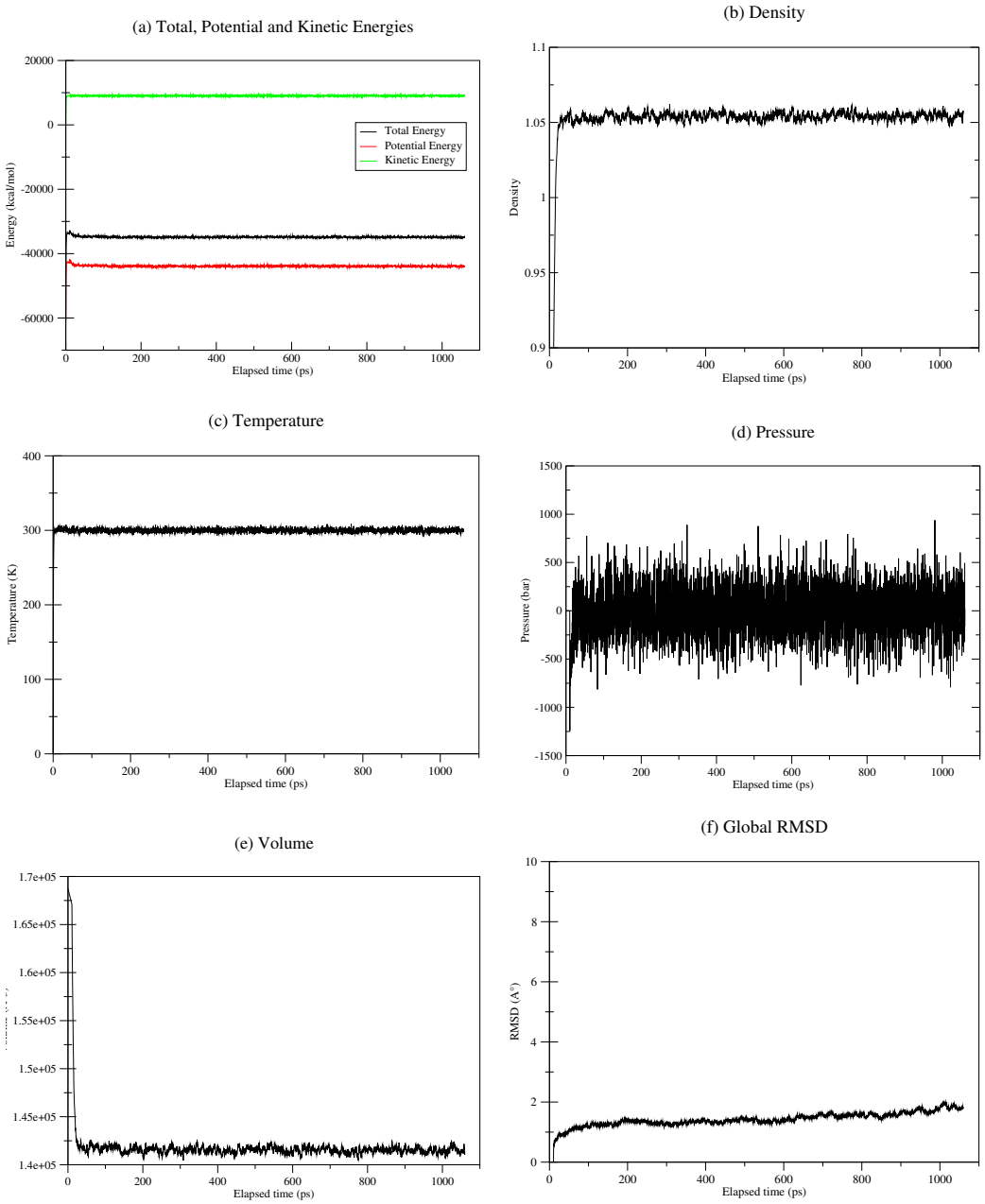

Figure S5: System properties as a function of time for Q61L NRas during QM/MM dynamics simulations (a) Potential, kinetic and total energy (b) Density, (c)Temperature, (d) Pressure, (e) Volume and (f) backbone atoms rmsd.

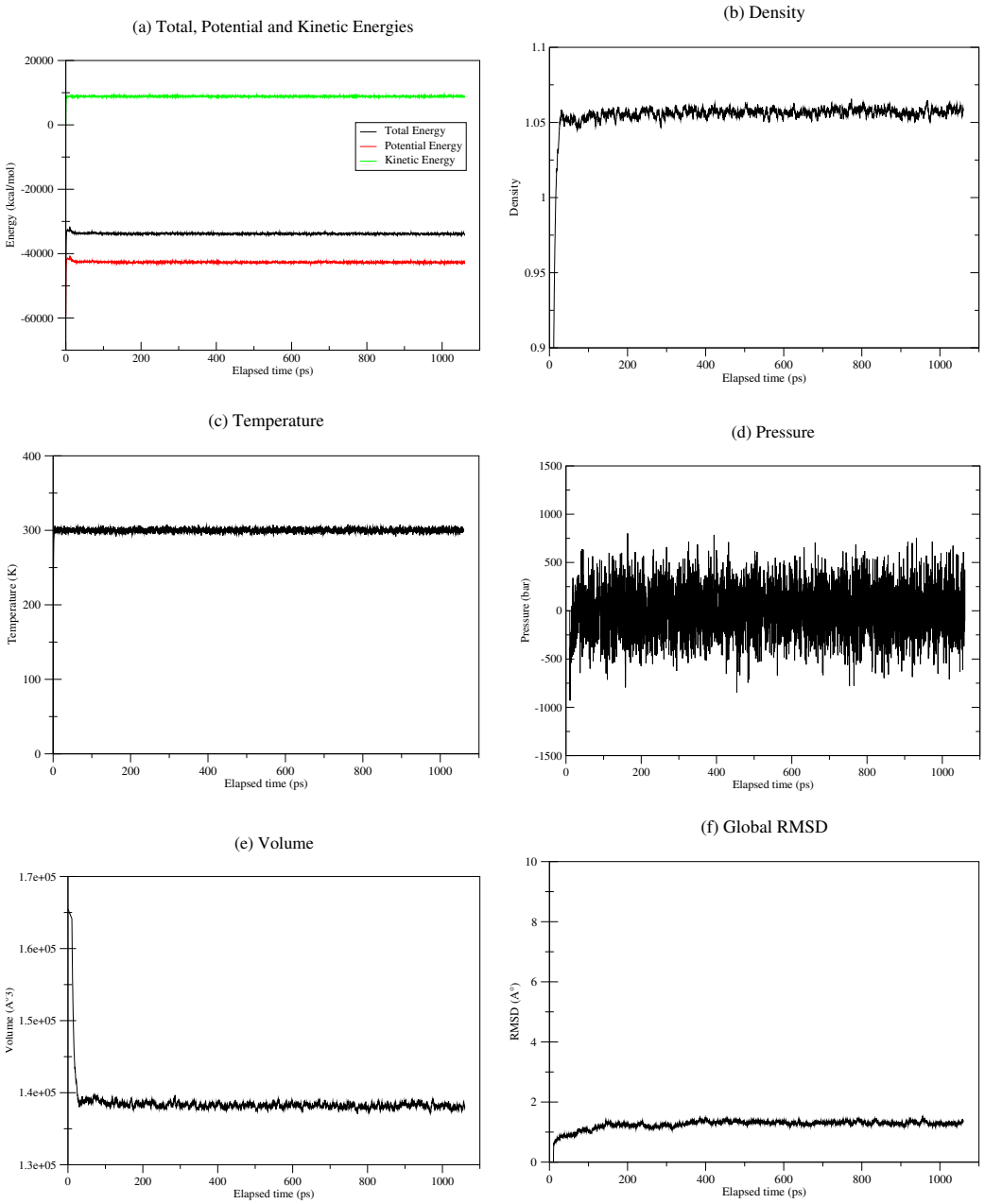

Figure S6: System properties as a function of time for Q61K NRas during QM/MM dynamics simulations (a) Potential, kinetic and total energy (b) Density, (c)Temperature, (d) Pressure, (e) Volume and (f) backbone atoms rmsd.

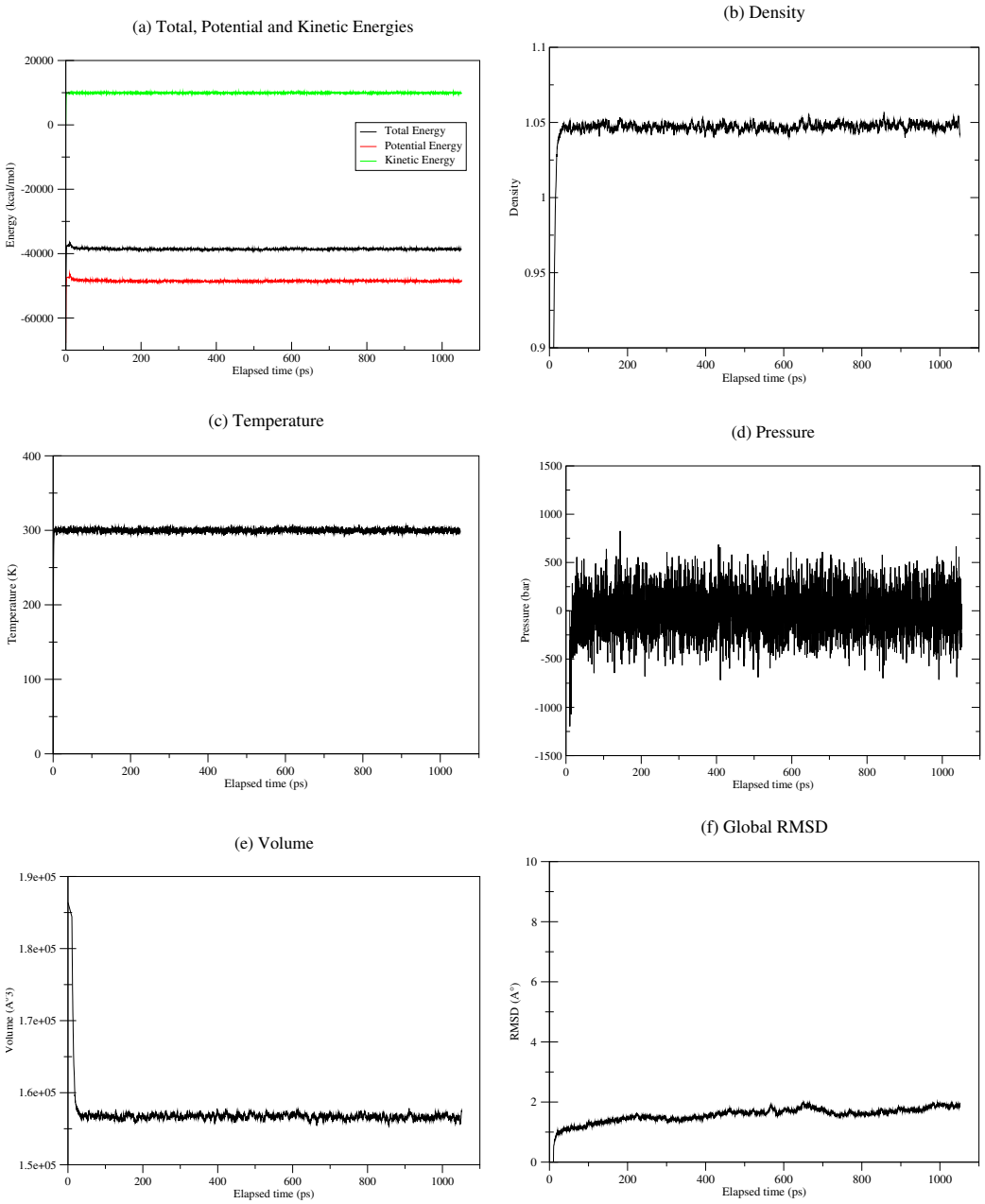

Figure S7: System properties as a function of time for Q61R NRas during QM/MM dynamics simulations (a) Potential, kinetic and total energy (b) Density, (c)Temperature, (d) Pressure, (e) Volume and (f) backbone atoms rmsd.

S1. Active site stability

Side chain RMSD plots

The structural impact of Gln 61 substitutions on NRas was assessed by computing the RMSD, with respect to the initial structure, of each residue forming the active site. This analysis was carried out for each individual side-chain. The fluctuations observed in the plots hence correspond to their intrinsic mobility. Figures S8 to S14 present the RMSD plot of residues that remain stable upon mutation, figures S15 to S19 present the RMSD plot of residues that undergo conformational changes within Q61E, Q61P, Q61H, Q61L and Q61K mutant proteins. For WT NRas and Q61R mutant, the most NRas widespread mutation, RMSD plots of the same mobile residues are found in figures 2 and 4 of the article, respectively.

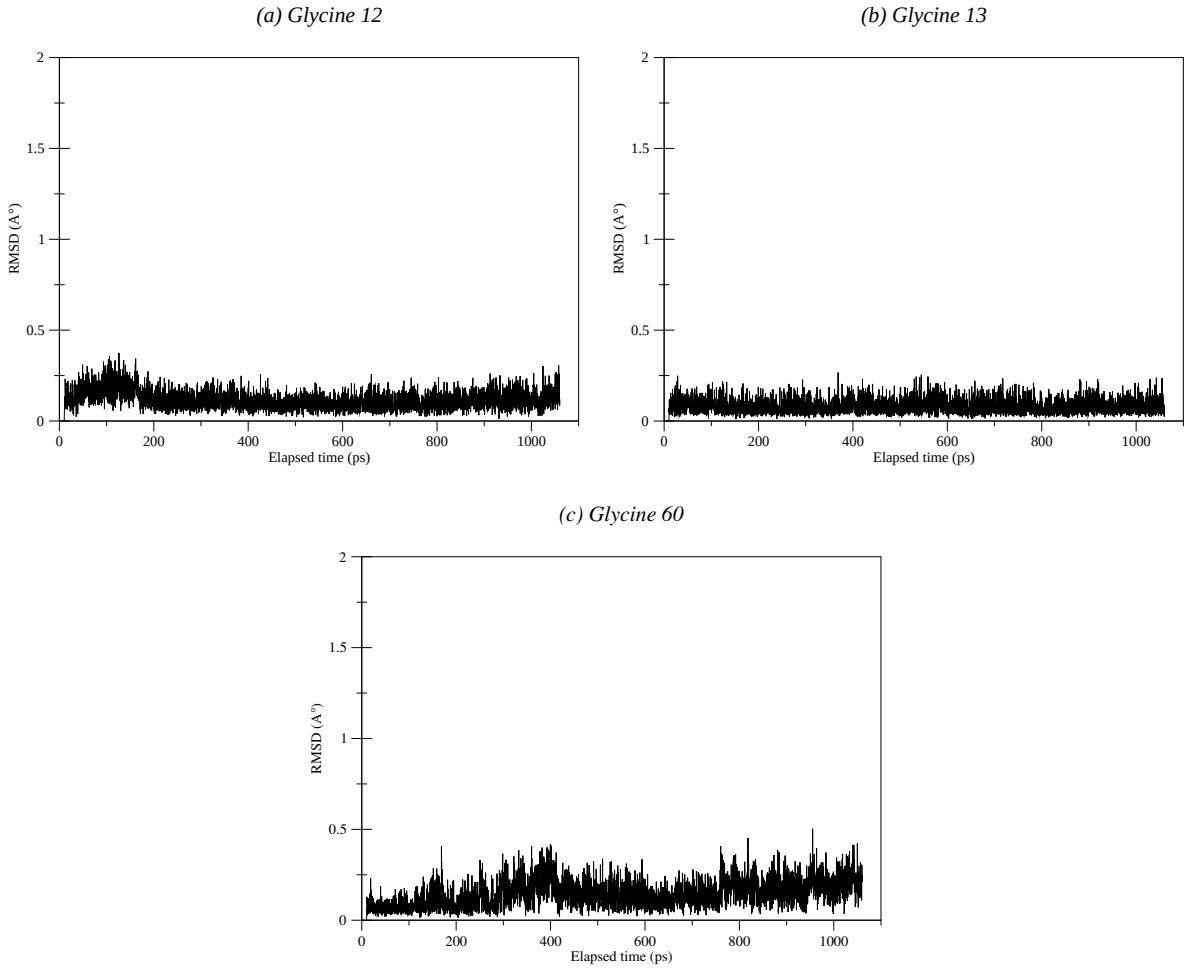

Figure S8: RMSD plot of *(a)* Glycine 12, *(b)* Glycine 13 and *(c)* Glycine 60 within the active site of wild-type p21^{N-ras} during QM/MM molecular dynamics

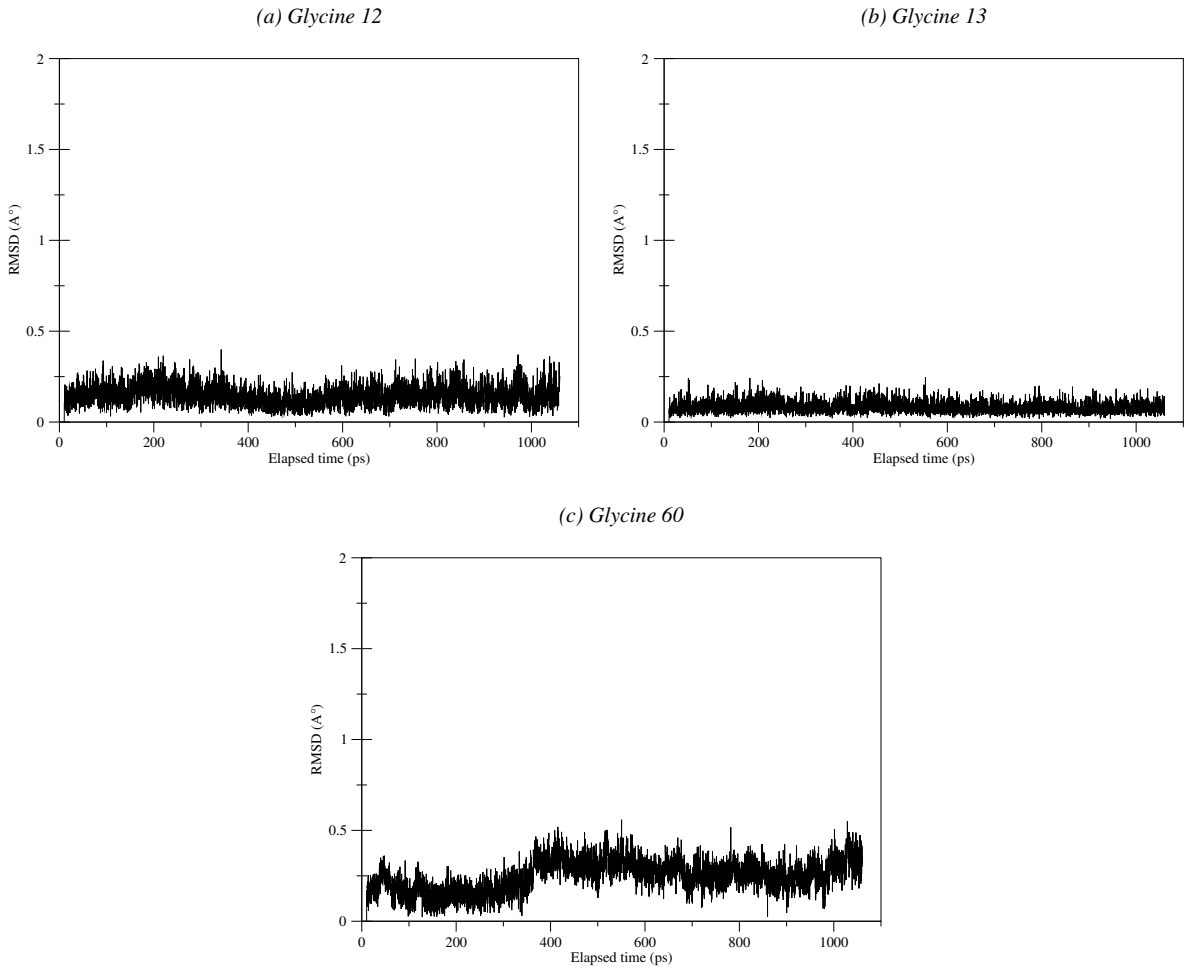

Figure S9: RMSD plot of *(a)* Glycine 12, *(b)* Glycine 13 and *(c)* Glycine 60 within the active site of Q61E NRas mutant during QM/MM molecular dynamics

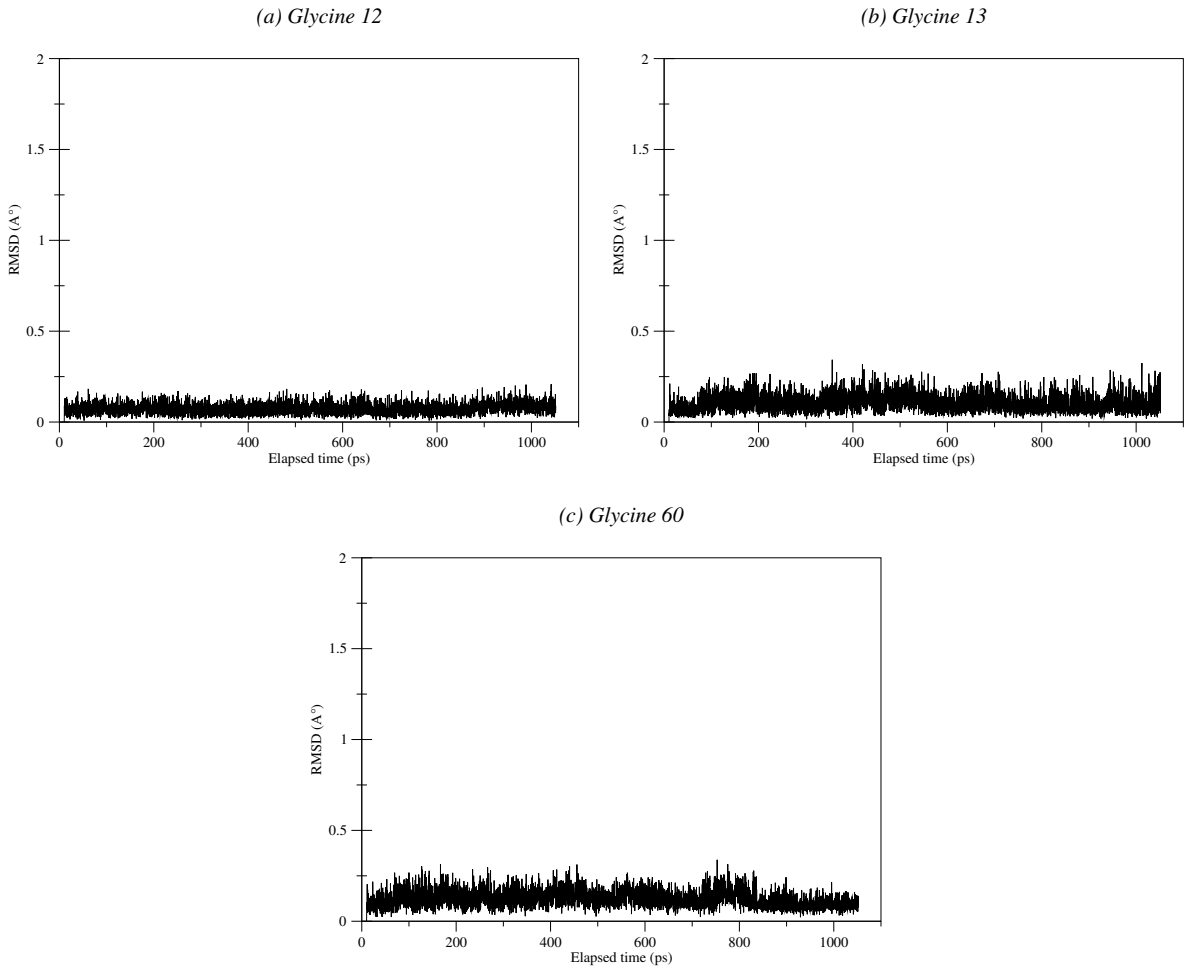

Figure S10: RMSD plot of *(a)* Glycine 12, *(b)* Glycine 13 and *(c)* Glycine 60 within the active site of Q61P NRas mutant during QM/MM molecular dynamics

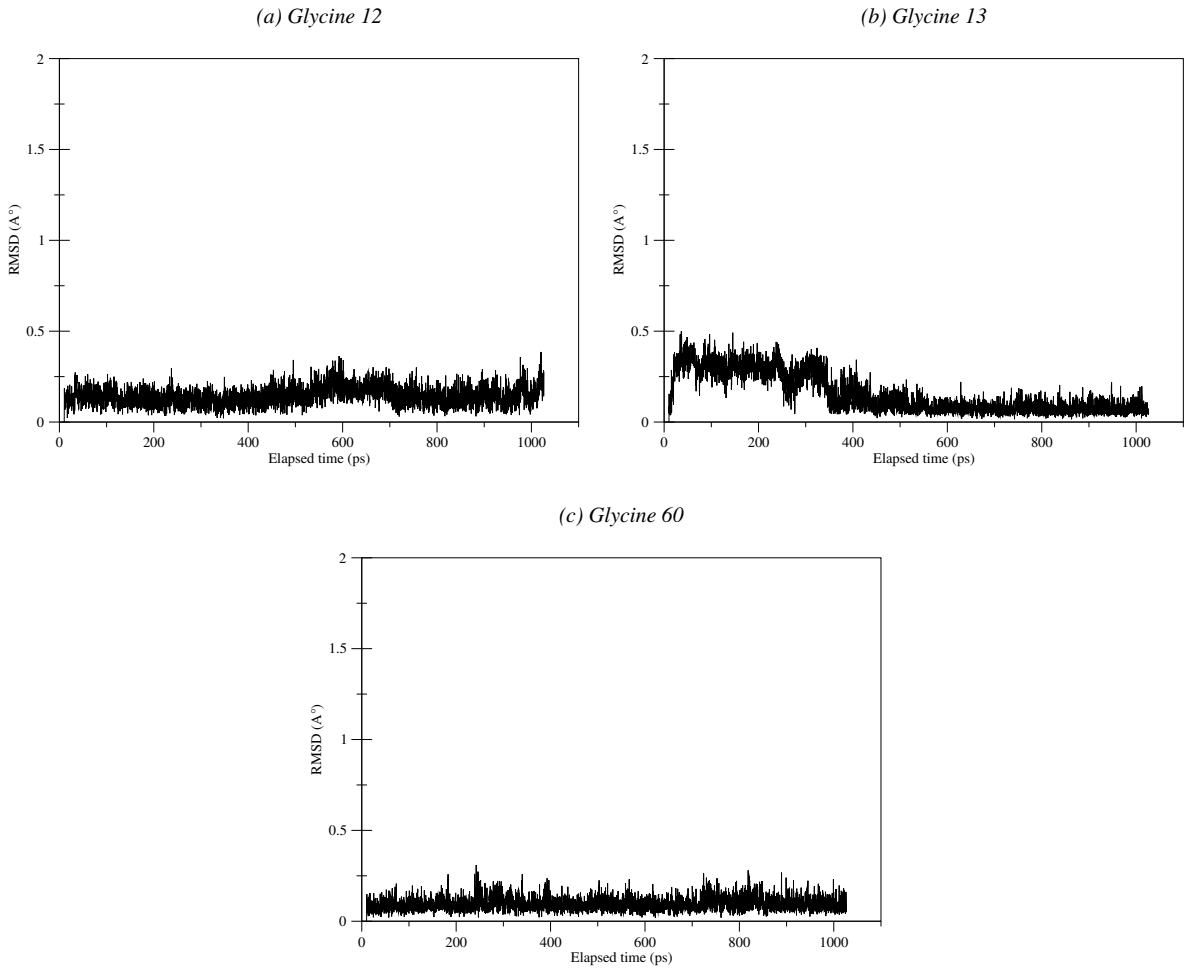

Figure S11: RMSD plot of *(a)* Glycine 12, *(b)* Glycine 13 and *(c)* Glycine 60 within the active site of Q61H NRas mutant during QM/MM molecular dynamics

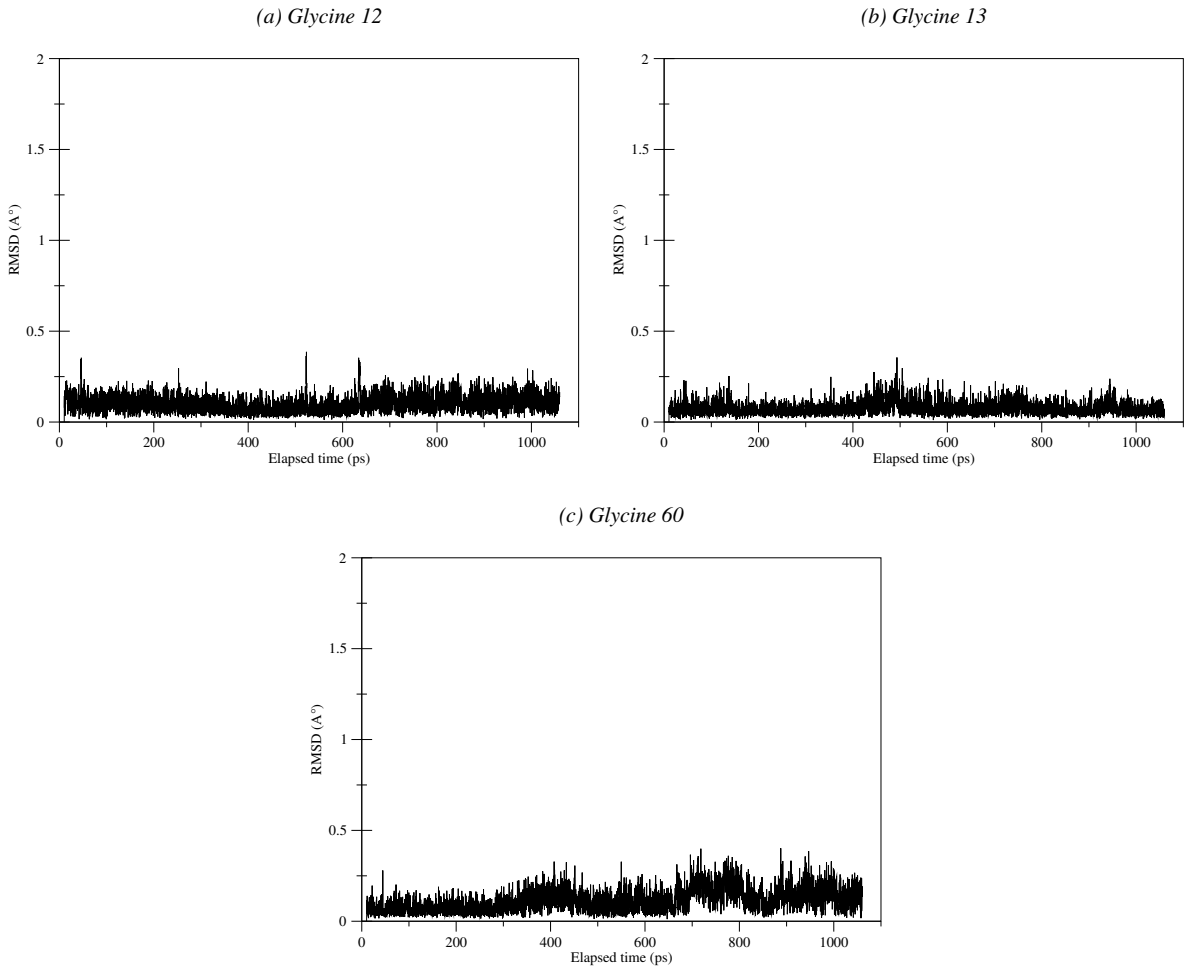

Figure S12: RMSD plot of *(a)* Glycine 12, *(b)* Glycine 13 and *(c)* Glycine 60 within the active site of Q61L NRas mutant during QM/MM molecular dynamics

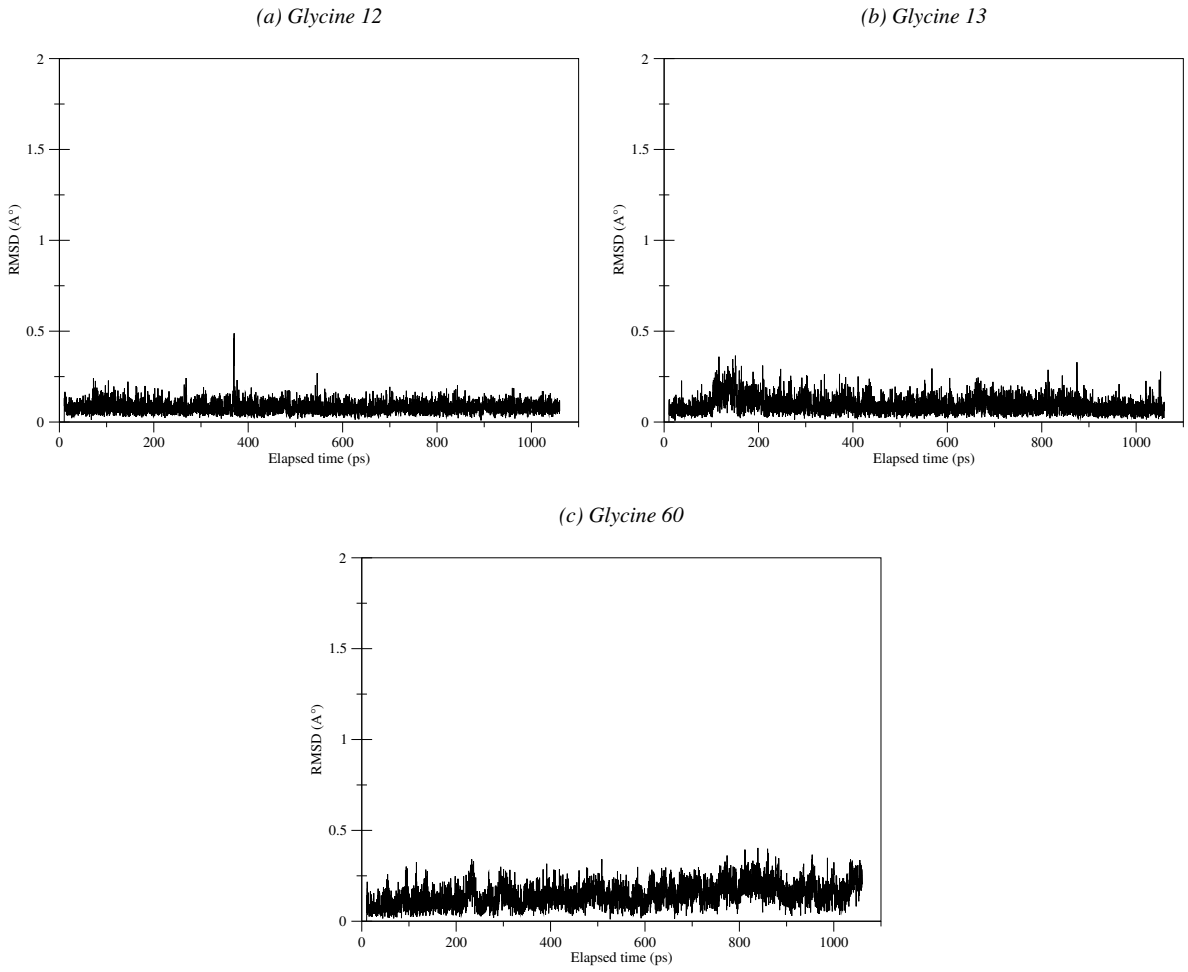

Figure S13: RMSD plot of *(a)* Glycine 12, *(b)* Glycine 13 and *(c)* Glycine 60 within the active site of Q61K NRas mutant during QM/MM molecular dynamics

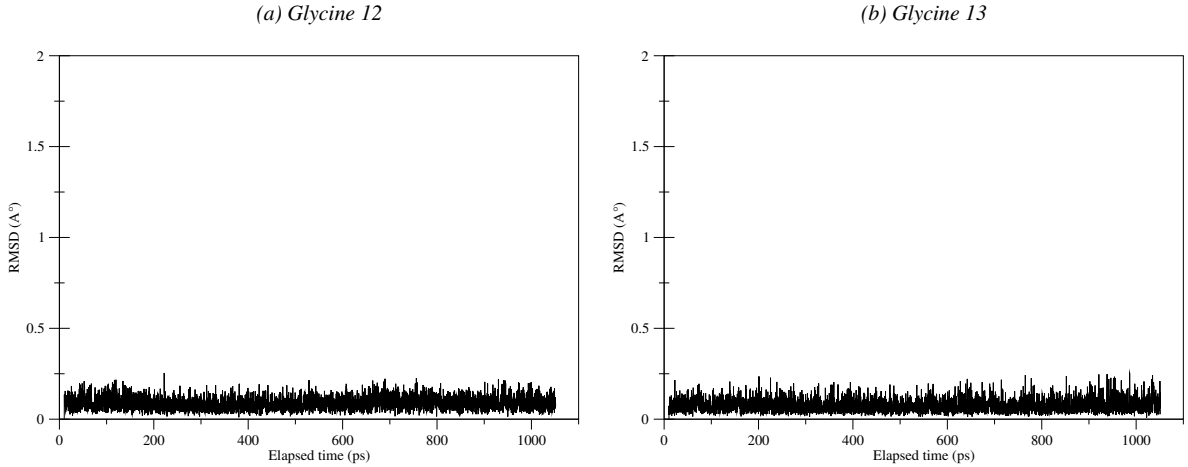

Figure S14: RMSD plot of *(a)* Glycine 12 and *(b)* Glycine 13 within the active site of Q61R NRas mutant during QM/MM molecular dynamics

Native/non-native contacts

Unlike NRas residues for which their side chain RMSD plot is sufficient to describe what we observe during the visualisation of the obtained trajectories, GAP Arg 789 behaviour is poorly depicted by this sort of analysis. In order to better depict the *arginine finger* behaviour, we propose to analyse the *native/non-native contacts* it engages in during the simulation.

The *native/non-native contacts* analysis consists in identifying possible interactions between two atoms based on a distance criterion. The *native contacts* are present in the initial structure while the *non-native contacts* are formed in the course of the simulation. After running this analysis, we have identified the strongest *native/non-native contacts* by i) searching for the ones that remain the longest, ii) identifying the atoms that have the most numerous *native/non-native contacts* with the arginine residue. Following this procedure, we have made the average of the *native/non-native contacts* of a given atom with the entire Arg 789 such that if a given atom has 9 contacts with Arg 789 (i.e. with 9 different atoms of Arg 789), then the plot of *native/non-native contacts* lifetime represents the average between the 9.

The corresponding figures are presented and discussed in figures 2*(d)* and 4*(d)* of the article for WT NRas and Q61R mutant, respectively. For Q61E, Q61P, Q61H, Q61L and Q61K they are presented in figures S15*(d)* to S19*(d)* and discussed in the article.

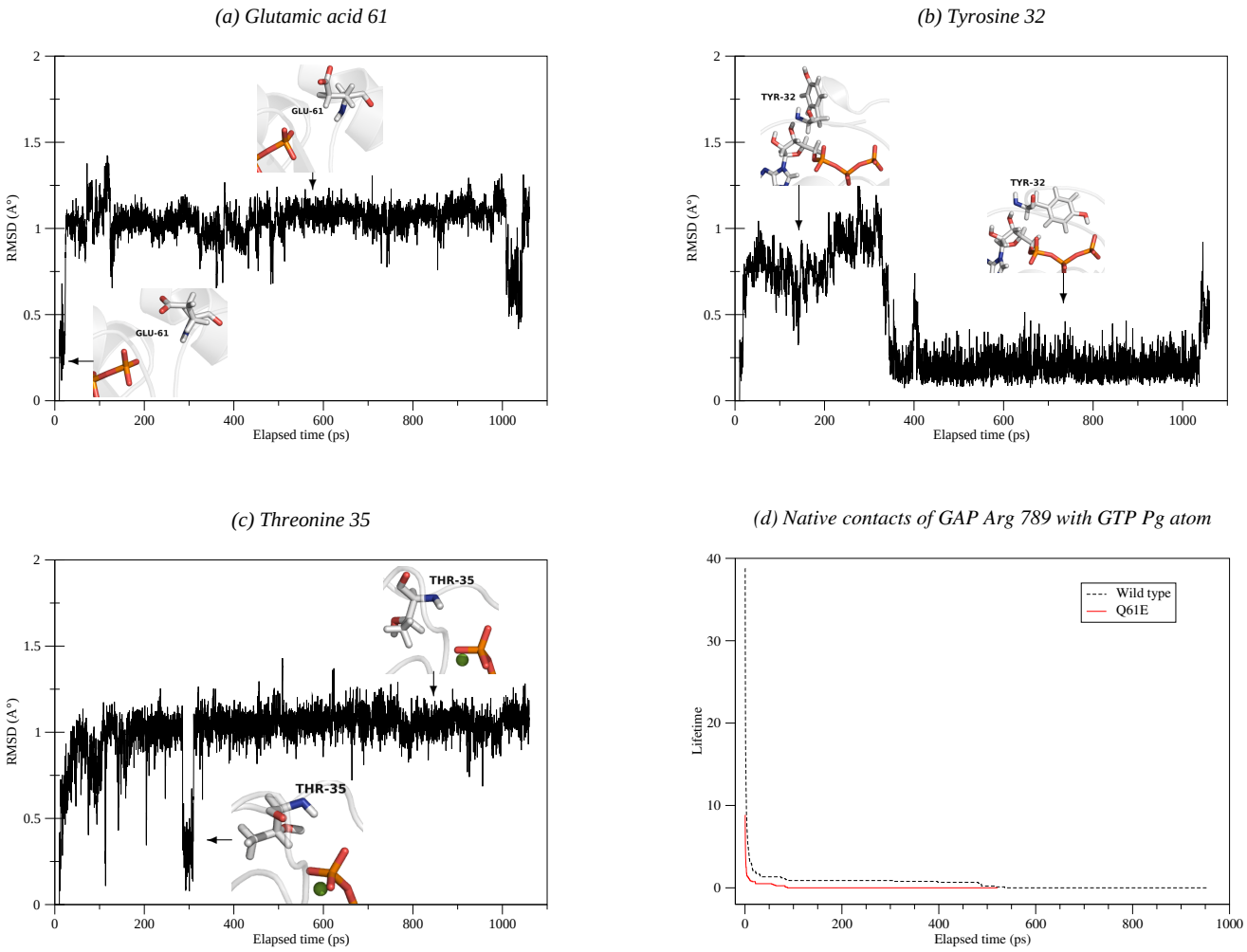

Figure S15: RMSD plots alongside the associated conformational changes of Glu 61 (a), Tyr 32 (b), Thr 35 (c) from Q61E NRas and lifetime curve of *native contacts* between GTP P_γ atom and GAP Arg 789 (d) during QM/MM molecular dynamics.

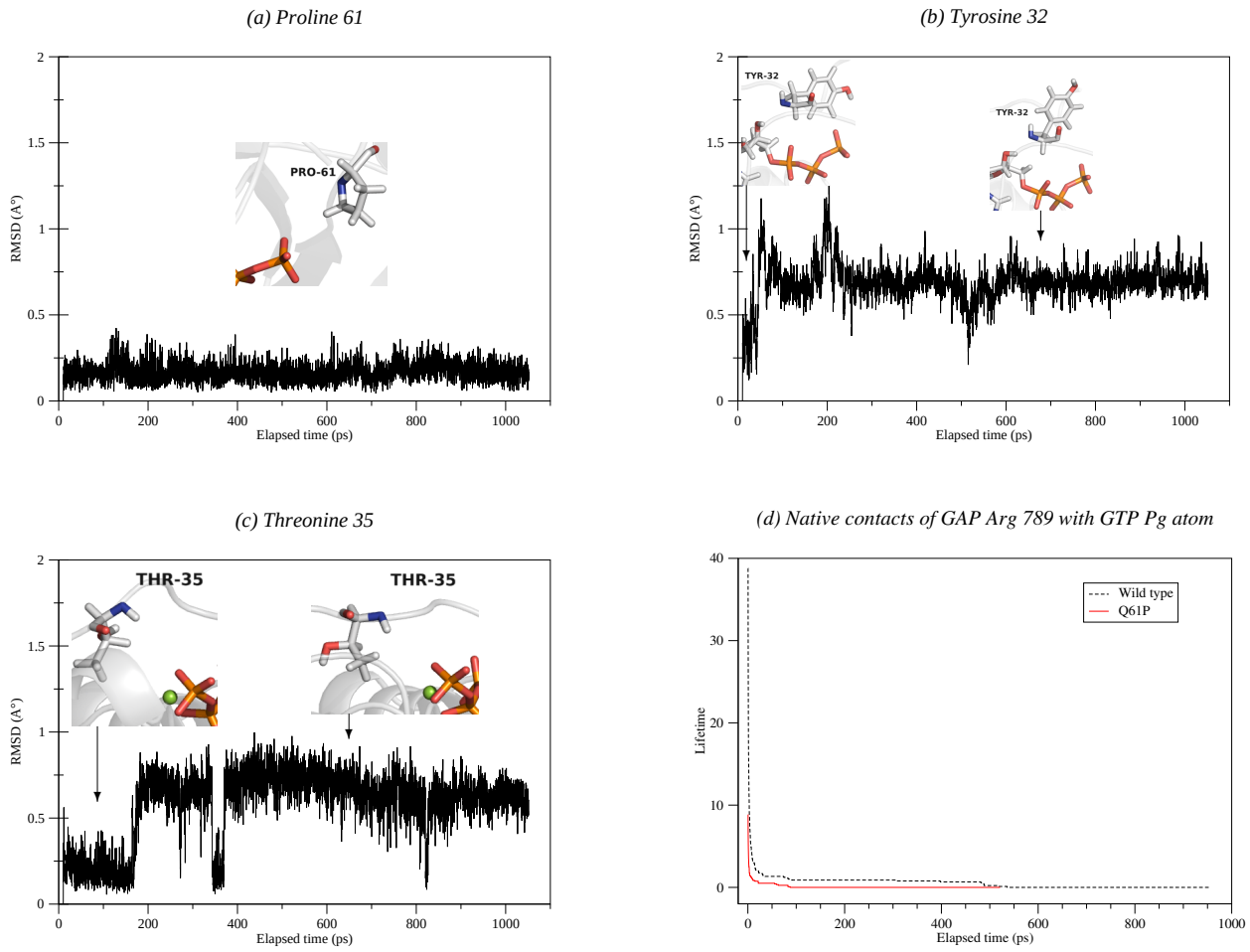

Figure S16: RMSD plots alongside the associated conformational changes of Pro 61 (a), Tyr 32 (b), Thr 35 (c) from Q61P NRas and lifetime curve of *native contacts* between GTP P_γ atom and GAP Arg 789 (d) during QM/MM molecular dynamics.

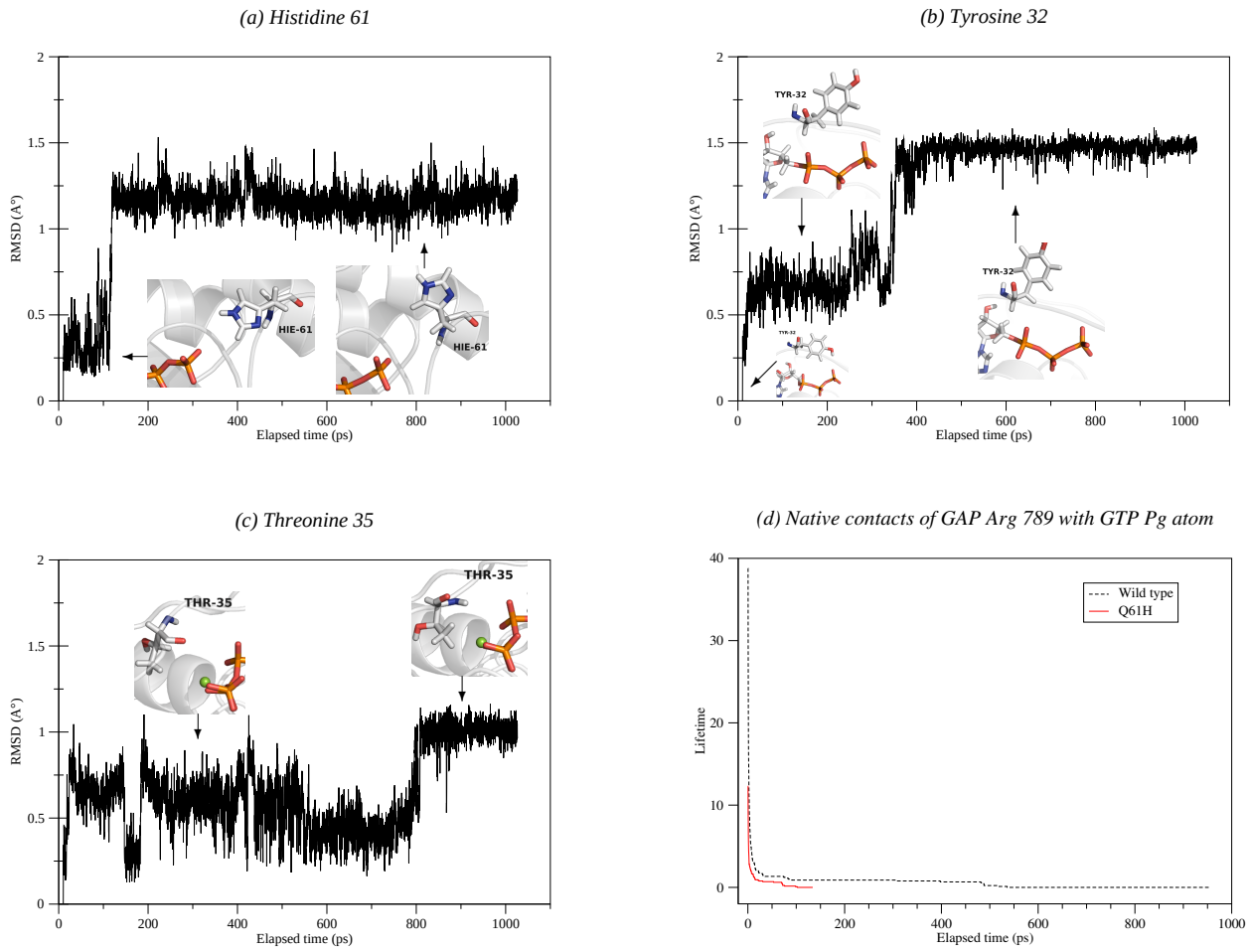

Figure S17: RMSD plots alongside the associated conformational changes of His 61 (a), Tyr 32 (b), Thr 35 (c) from Q61H NRas and lifetime curve of *native contacts* between GTP P_γ atom and GAP Arg 789 (d) during QM/MM molecular dynamics.

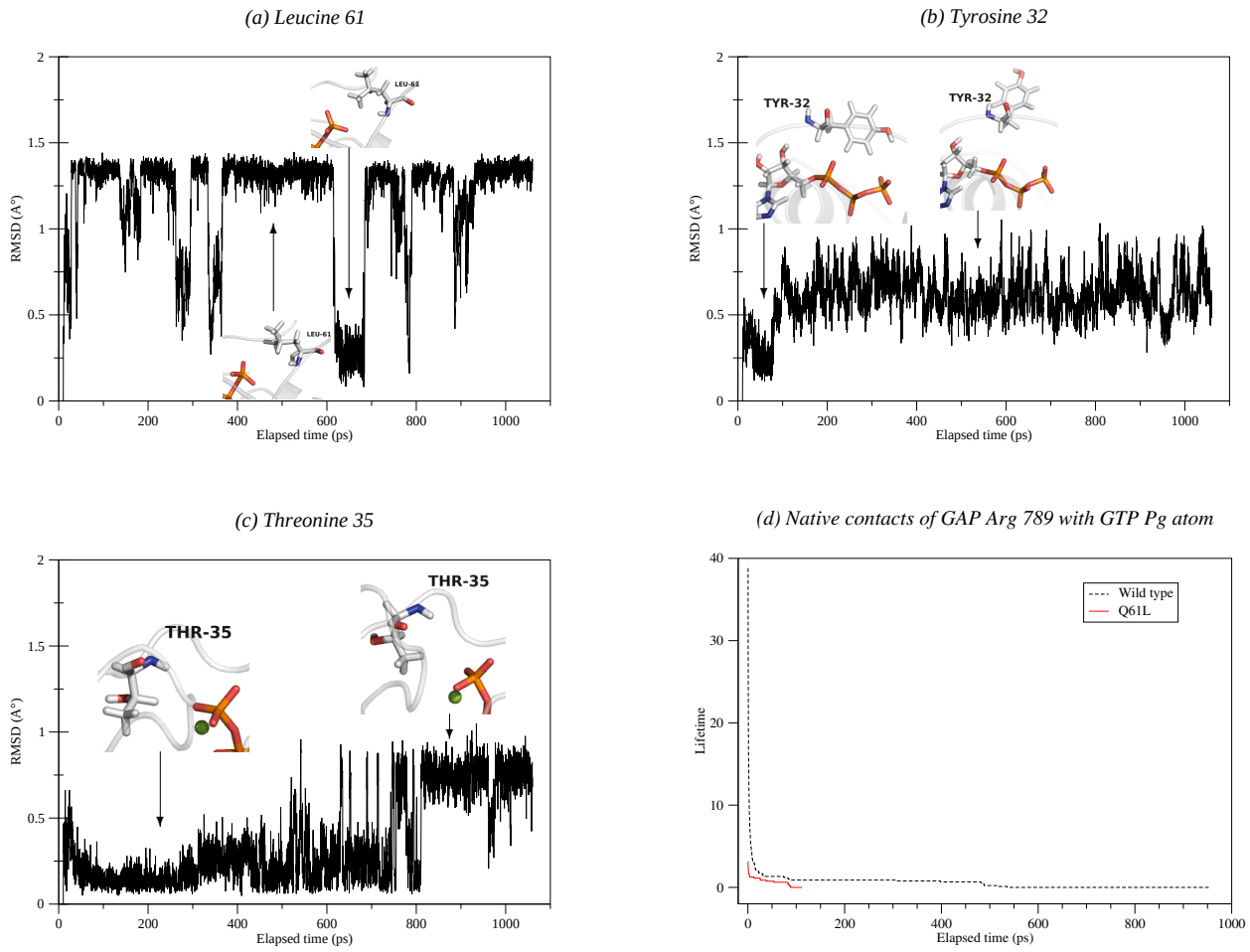

Figure S18: RMSD plots alongside the associated conformational changes of Leu 61 (a), Tyr 32 (b), Thr 35 (c) from Q61L NRas and lifetime curve of *native contacts* between GTP P_γ atom and GAP Arg 789 (d) during QM/MM molecular dynamics.

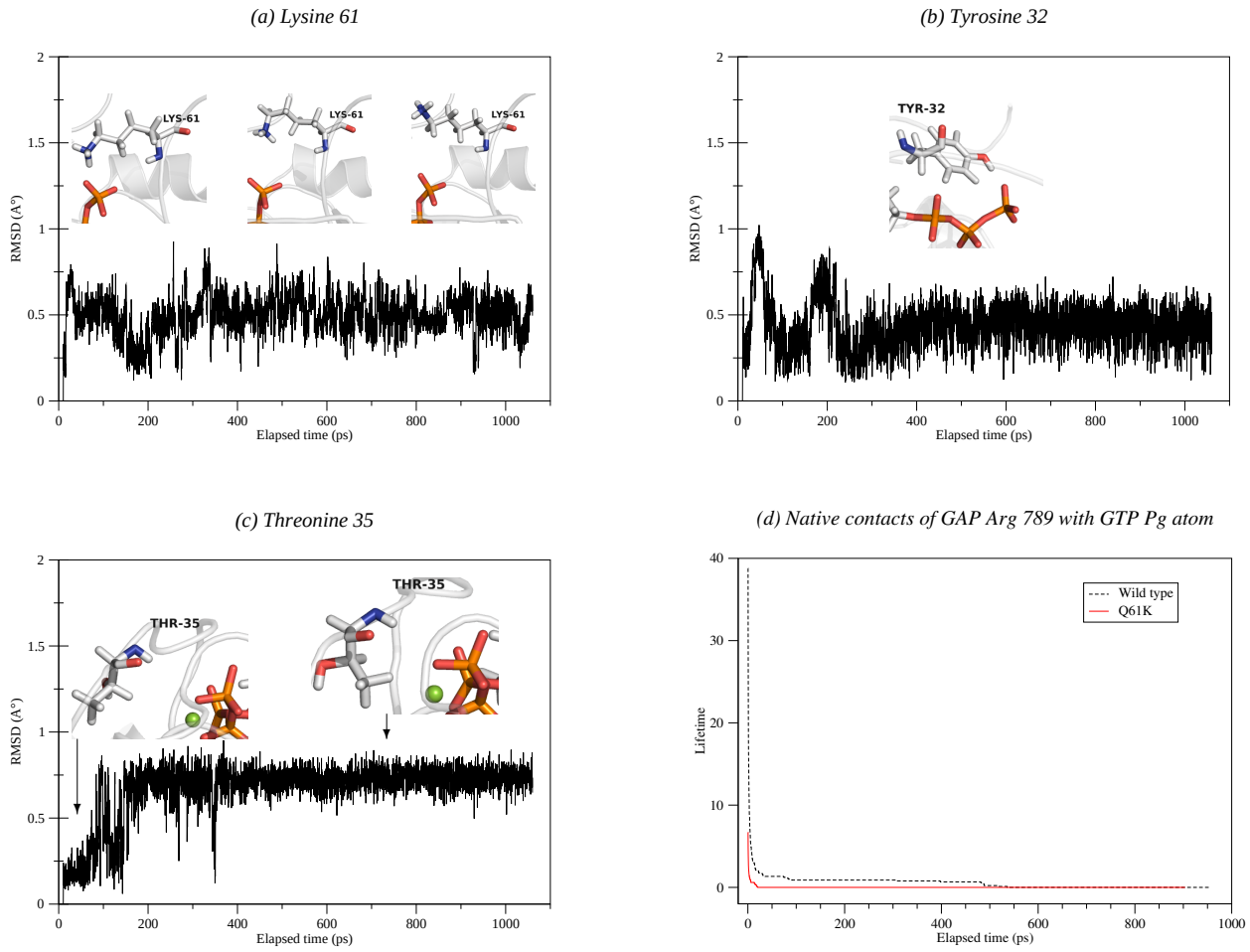

Figure S19: RMSD plots alongside the associated conformational changes of Lys 61 (a), Tyr 32 (b), Thr 35 (c) from Q61K NRas and lifetime curve of *native contacts* between GTP P_γ atom and GAP Arg 789 (d) during QM/MM molecular dynamics.

S2. 2D RDF algorithm

We implemented an algorithm with the objective of mapping water molecules occupancy in the protein active site. The developed algorithm counts the number of water molecules as a function of the distance from a given atom and subsequently projects them on a plane of interest. To define this plane, an orthonormal basis, based on three atoms coordinates, is chosen at the beginning of the simulation run or for each new generated configuration. In the later case, the changes of the coordinates of the three reference atoms are taken into account.

In this study, we considered that a plane containing GTP P_β and P_γ atoms was the most appropriated to describe water occupancy in NRas active site. Three GTP atoms, P_β, P_γ and $O_{1\gamma}$ (see figure S20), were chosen to define the orthonormal basis. The first vector is normalized $\overrightarrow{P_\beta P_\gamma}$. The second vector is built from the orthogonal projection of $O_{1\gamma}$ coordinates on the plane containing P_γ atom and to which $\overrightarrow{P_\beta P_\gamma}$ is a normal vector. We thus define and normalize the second vector $\overrightarrow{P_\gamma O_{1\gamma p}}$, where $O_{1\gamma p}$ is the orthogonal projection of $O_{1\gamma}$. Finally, the third vector of this orthonormal basis is obtained by the cross product of $\overrightarrow{P_\beta P_\gamma}$ and $\overrightarrow{P_\gamma O_{1\gamma p}}$. On the plane perpendicular to $\overrightarrow{P_\gamma O_{1\gamma p}}$, we projected on water molecules found within 7 Å of GTP P_γ atom, as well as noticeable atoms of the active site to locate where water molecules have the highest probability to stay relative to these atoms. We chose to center the plane at P_γ.

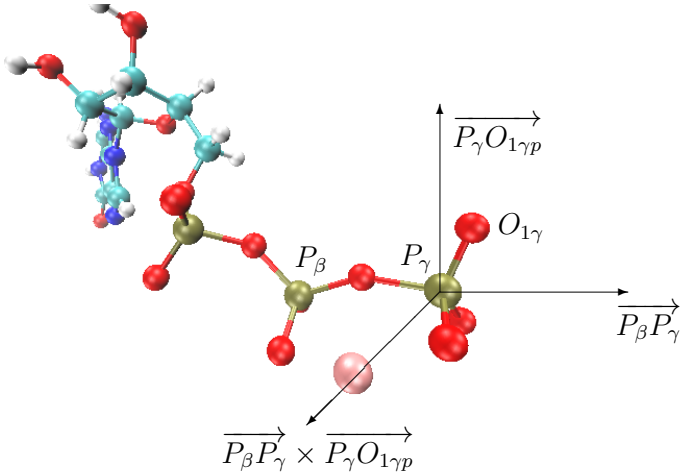

Figure S20: Orthonormal basis defined by GTP P_β, P_γ and $O_{1\gamma}$ atoms

	WT		Q61E		Q61P		Q61H		Q61L		Q61K		Q61R	
Residue	Conformations	Stability	Conformations	Stability	Conformations	Stability	Conformations	Stability	Conformations	Stability	Conformations	Stability	Conformations	Stability
Gly 12	cristallographic	S	cristallographic	S	cristallographic	S	cristallographic	S	cristallographic	S	cristallographic	S	cristallographic	S
Gly 13	cristallographic	S	cristallographic	S	cristallographic	S	cristallographic	S	cristallographic	S	cristallographic	S	cristallographic	S
Tyr 32	open	s	closed	s	open	s	open	s	open	s	closed	s	open	s
Thr 35	HO in, CH_3 out HO out, CH_3 in CH_3 w/ Mg^{2+}	S	HO in, CH_3 out HO out, CH_3 in	S	HO out, CH_3 in CH_3 w/ Mg^{2+}	S	HO in, CH_3 out HO out, CH_3 in CH_3 w/ Mg^{2+}	S	HO in, CH_3 out HO out, CH_3 in HO out, CH_3 out	S	HO out, CH_3 in HO out, CH_3 out	S	HO in, CH_3 out HO out, CH_3 in HO out, CH_3 out	u
Ala 59	cristallographic	S	cristallographic	S	cristallographic	S	cristallographic	S	cristallographic	S	cristallographic	S	cristallographic	S
Gly 60	cristallographic	S	cristallographic	S	cristallographic	S	cristallographic	S	cristallographic	S	cristallographic	S	h-bonds w/ Thr 791	u
61	open	s	open bent to GTP	s	crystallographic	s	open bent to GTP	s	1 CH_3 to GTP 2 CH_3 to GTP	u	closed	s	open	u
RDF	Peak Distance Ampl	Integral 5Å 7Å	Peak Distance Ampl	Integral 5Å 7Å	Peak Distance Ampl	Integral 5Å 7Å	Peak Distance Ampl	Integral 5Å 7Å	Peak Distance Ampl	Integral 5Å 7Å	Peak Distance Ampl	Integral 5Å 7Å	Peak Distance Ampl	Integral 5Å 7Å
P_α	—	0 0.20	3.9 Å 0.02	0.18 1.33	3.9 Å 0.10	0.66 2.41	3.7 Å 0.07	0.53 1.62	3.8 Å 0.06	0.55 1.64	—	0.02 0.76	4.0 Å 0.27	1.35 3.43
P_γ	3.8Å 0.21	1.52 3.42	4.0 Å 0.22	1.56 4.46	4.0 Å 0.14	0.99 2.78	3.8 Å 0.36	2.32 5.05	4.0 Å 0.15	1.03 3.54	3.8 Å 0.25	1.17 3.68	4.0 Å 0.24	1.50 5.33
2D RDF	Arch	2.63 3.35	Delocalised	3.33 4.46	Delocalised Arch	2.12 2.77	Localised	4.17 5.05	Delocalised	2.80 3.54	Localised	2.70 3.68	Delocalised	4.34 5.33

Table 1: Main conformation(s) and general stability of residues forming the active site along RDF and 2D RDF of water molecules within WT NRas and Q61 NRas mutants. In the stability column, s denotes *stable residue* and u *unstable residue*. The 2D RDF integrals are calculated for P_γ centered squares which borders extend up to 5Å and 7Å away from GTP P_γ atom